Systematic Study of Mn-Doping Trends in Optical Properties of (Ga,Mn)As

T. Jungwirth,[1,2] P. Horodyská,[3] N. Tesařová,[3] P. Němec,[3] J. Šubrt,[3] P. Malý,[3] P. Kužel,[4] C. Kadlec,[4] J. Mašek,[4] I. Němec,[5] M. Orlita,[6,1] V. Novák,[1] K. Olejník,[1,7] Z. Šobáň,[1,8] P. Vašek,[1] P. Svoboda,[1] and Jairo Sinova[9,1]

[1]*Institute of Physics ASCR, v.v.i., Cukrovarnická 10, 162 53 Praha 6, Czech Republic*
[2]*School of Physics and Astronomy, University of Nottingham, Nottingham NG7 2RD, United Kingdom*
[3]*Faculty of Mathematics and Physics, Charles University in Prague, Ke Karlovu 3, 121 16 Prague 2, Czech Republic*
[4]*Institute of Physics ASCR, v.v.i., Na Slovance 2, 182 21 Prague 8, Czech Republic*
[5]*Faculty of Science, Charles University in Prague, Hlavova 2030, 128 40 Prague 2, Czech Republic*
[6]*Laboratoire National des Champs Magnétiques Intenses, CNRS-UJF-UPS-INSA, 25, avenue des Martyrs, 38042 Grenoble, France*
[7]*Hitachi Cambridge Laboratory, Cambridge CB3 0HE, United Kingdom*
[8]*Faculty of Electrical Engineering, Czech Technical University in Prague, Technická 2, 166 27 Prague, Czech Republic*
[9]*Department of Physics, Texas A&M University, College Station, Texas 77843-4242, USA*

(Received 28 July 2010; revised manuscript received 8 October 2010; published 23 November 2010)

We report on a systematic study of optical properties of (Ga,Mn)As epilayers spanning the wide range of accessible Mn_{Ga} dopings. The material synthesis was optimized for each nominal Mn doping in order to obtain films which are as close as possible to uniform uncompensated (Ga,Mn)As mixed crystals. We observe a broad maximum in the mid-infrared absorption spectra whose position exhibits a prevailing blueshift for increasing Mn doping. In the visible range, a peak in the magnetic circular dichroism also shifts with increasing Mn doping. The results are consistent with the description of ferromagnetic (Ga,Mn)As based on the microscopic valence band theory. They also imply that opposite trends seen previously in the optical data on a limited number of samples are not generic and cannot serve as an experimental basis for postulating the impurity band model of ferromagnetic (Ga,Mn)As

DOI: 10.1103/PhysRevLett.105.227201 PACS numbers: 75.50.Pp, 71.55.Eq, 75.30.−m, 75.70.Ak

The discovery of ferromagnetism in (Ga,Mn)As above 100 K [1] opened an attractive prospect for exploring the physics of magnetic phenomena in doped semiconductors and for developing advanced concepts for spintronics. Assessment of a wide range of magnetic and transport properties of the material [2–4] showed that in ferromagnetic (Ga,Mn)As with Mn dopings $x > 1\%$, disorder-broadened and shifted host Bloch bands represent a useful one-particle basis for describing this mixed-crystal degenerate semiconductor. The common kinetic-exchange model implementation of this valence band theory and the more microscopic tight-binding Anderson model or *ab initio* density functional theory can all be shown [5] to be mutually consistent on the level of atomic and orbital resolved band structure. The main utility of valence band theories has been in providing a qualitative and often semiquantitative description of phenomena originating from the exchange split and spin-orbit coupled electronic structure and in assisting the development of prototype spintronic devices [4].

In the insulator nonmagnetic regime ($x \ll 1\%$), the system is readily described by localized Fermi level states residing inside a narrow impurity band separated from the valence band by an energy gap of magnitude close to the isolated Mn_{Ga} impurity binding energy. Recently, a debate has been stirred by proposals, based in particular on optical spectroscopy measurements [6], that the narrow impurity band persists in high-doped (Ga,Mn)As with metallic conduction.

Several phenomenological variants of the impurity band model have been proposed for the high-doped regime [6–10] which are mutually inconsistent from the perspective of the assumed atomic orbital nature of the impurity band states [5]. Further theoretical inconsistencies have arisen from attempts to recreate the phenomenological models microscopically with the constraint of the experimentally determined moderate binding energy of an isolated Mn_{Ga} of $E_a = 0.1$ meV. A detached narrow impurity band does not persist in any of the variants of the model to dopings $x > 1\%$ at which (Ga,Mn)As has metallic conduction [5]. Since to date no framework has been introduced which would allow us to test the validity of the impurity band model by comparing microscopic theory calculations to experiment, it is only the experimental evidence alone which can serve as a basis for postulating the impurity band picture. In particular, the redshift of the infrared absorption peak and the rigidity of the near band-gap spectral features in the magnetic circular dichroism with increasing doping [6,7,9] have been regarded as the key experimental signatures of the impurity band. The goal of this Letter is to assess whether these signatures are generic in ferromagnetic (Ga,Mn)As materials to represent a valid experimental foundation of the impurity band model. Simultaneously we inspect the consistency of the valence band theory of (Ga,Mn)As with the measured data.

We study doping trends in the optical spectra over a wide Mn concentration range in a consistently and controllably prepared set of materials. We have optimized the growth

and postgrowth annealing procedures individually for each nominal doping in order to minimize the density of compensating defects and other unintentional impurities and to achieve high uniformity of the epilayers in the growth and lateral directions, as detailed in the supplementary material [11]. Nominal dopings of our set of (Ga,Mn)As epilayers grown on GaAs substrates span a range from paramagnetic insulating materials with $x < 1\%$ to materials with x up to $\approx 14\%$, corresponding to $\approx 8\%$ of uncompensated Mn_{Ga}, and ferromagnetic transition temperatures reaching 190 K [11]. Samples with $x \leq 1\%$ have thickness of 100 nm. All epilayers with $x \geq 1.5\%$ are 20 nm thick. In these materials with large Mn doping, high quality epilayers are obtained only for thicknesses larger than ~10 nm and lower than ~50 nm. All samples within the series have reproducible characteristics with the overall trend of increasing Curie temperature (in the ferromagnetic films), increasing hole concentration, and increasing magnetic moment density with increasing x. The samples have a high degree of uniformity on a macroscopic scale as inferred from their sharp magnetic and transport singularities at the Curie point (see supplementary material for more details [11]).

Samples used in transmission measurements have a polished back side of the wafers to minimize diffusive light scattering. The unpolarized transmission experiments [11] on the (Ga, Mn)As/GaAs samples and on the control bare GaAs substrate were performed at 300 K in the range 25–11 000 cm^{-1} (3–1360 meV) using the Fourier transform infrared spectroscopy. The range between 120–600 cm^{-1} (15–75 meV) with strong phonon response in GaAs substrate is excluded from the data. Control low-temperature measurements which confirm the doping trends observed at 300 K are included in the supplementary material [11]. Measurements of the complex conductivity in the low-frequency range 8–80 cm^{-1} (1–10 meV) of the (Ga, Mn)As/GaAs wafers (with measurement of the bare GaAs substrate as a reference) were performed by means of terahertz time-domain transmission spectroscopy [11]. Magneto-optical experiments [11] at 15 K in the near infrared to visible range 970–20160 cm^{-1} (1.2–2.5 eV) were performed primarily in the reflection geometry because of the small epilayer thickness of the optimized materials and increasing growth strain in the (Ga, Mn)As/GaAs epilayers reaching 0.5% in the high-doped materials. Control magneto-optical measurements in transmission were done on a 230 nm thick (Ga,Mn)As epilayer with the GaAs substrate removed after growth by wet etching.

First we discuss the observed broad maximum in the unpolarized infrared absorption near 200 meV. In Fig. 1(a) we plot experimental data obtained directly from the measured infrared transmissivities. The real part of the ac conductivity curves shown in Fig. 1(b) represent the best fit to the measured transmission in the THz and infrared ranges [11]. The fit is anchored at low frequencies by the directly measured THz conductivity. (The scatter in the measured THz conductivity reflects the precision of these measurements which is limited primarily by the quality of sample surfaces [11].) The position of the midinfrared absorption peak in both representations of the measured data has a prevailing blueshift tendency with increasing doping. This is reminiscent of the blueshift of this spectral feature seen in our (and previously studied [12]) control GaAs:C materials, shown in Fig. 1(c). We recall that for the nonmagnetic hydrogenic acceptors it is established that the peak originates from transitions inside the semiconductor valence band. Based on microscopic valence band theory calculations, these transitions have also been predicted to

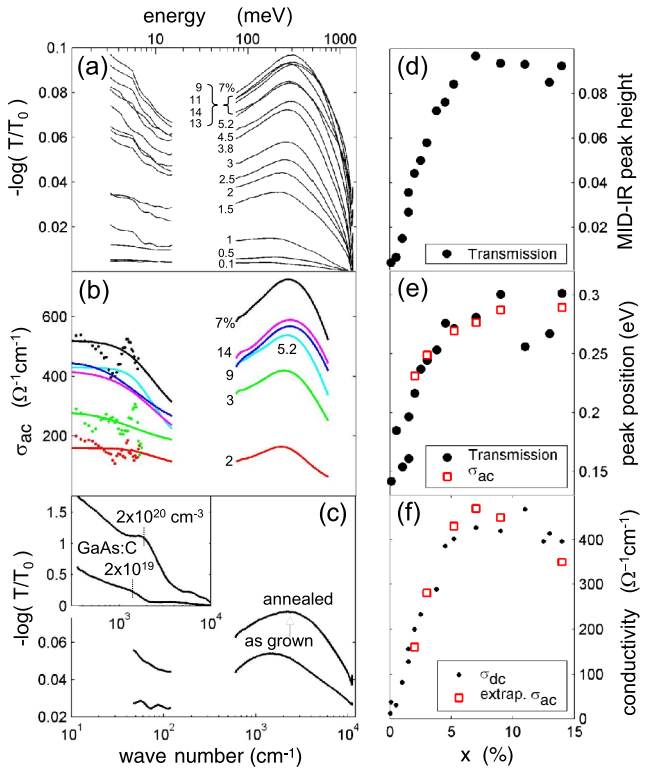

FIG. 1 (color online). (a) Infrared absorption of a series of optimized (Ga, Mn)As/GaAs epilayers with nominal Mn doping $x = 0.1\%$–14% plotted from the measured optical transmissions of the samples (T) and of the reference bare GaAs substrate (T_0). Spectra of the 100 nm thick samples with $x \leq 1\%$ were divided by 5 for consistency with those measured for the 20 nm thick higher doped samples. (b) Real part of the ac conductivity (lines) obtained from the measured complex conductivity in the terahertz range (points) and from fitting the complex conductivity in the infrared range to the measured transmissions. (c) Comparison of the infrared absorption in as-grown and annealed 4.5% doped sample. Inset: Comparison to GaAs:C samples with carbon doping densities 2×10^{19} and 2×10^{20} cm^{-3}. (d) Height of the (Ga,Mn)As midinfrared absorption peak as a function of Mn doping. (e) Position of the peak inferred from the transmission measurements and from the fitted ac conductivities. (f) Zero frequency conductivities obtained from dc-transport measurements and from extrapolated optical ac conductivities measured in the terahertz range.

yield the broad maximum in the midinfrared spectra of (Ga,Mn)As which is rather insensitive to the exchange splitting of the valence band [13,14]. Apart from the predicted prevailing blueshift, the peak position in (Ga,Mn)As can have a nonmonotonic dependence on doping as a consequence of momentum nonconserving transitions allowed by the strong disorder in (Ga,Mn)As [15].

A redshift of the measured midinfrared peak reported in Ref. [7] in as-grown and annealed samples arranged by expected increasing hole concentrations has been presented as the key evidence of the failure of the valence band theories. The data were phenomenologically interpreted in terms of impurity band conduction persisting to the high-doped metallic (Ga,Mn)As. In the subsequent analysis it has been pointed out [15], however, that the association of this peak to an impurity band is implausible (i) because of the absence of the thermally activated dc-transport counterpart in the high-doped samples, (ii) because of the initial blueshift of this midinfrared feature with respect to the impurity band transition peak in the very dilute insulating samples, and (iii) because of the appearance of the peak at frequencies above $2E_a$, which is the expected upper bound for impurity band transitions. Our data in Fig. 1 corroborate the conclusions of Ref. [15] by demonstrating that the redshift of the midinfrared peak with increasing Mn_{Ga} doping is not the general and not even the prevailing trend in (Ga,Mn)As materials prepared with the minimized number of compensating and other unintentional impurities.

In Figs. 1(a) and 1(b) we have not included measurements in the as-grown epilayers because their characteristics are not fully reproducible, are more ambiguous, and the materials are less uniform [11]. Nevertheless, to make a connection to previous studies we have measured the midinfrared peak in a nominally 4.5% Mn-doped sample before and after annealing. As shown in Fig. 1(c), we observe a blueshift of the midinfrared peak after annealing; i.e., the redshift is not observed in our materials even if we use annealing to increase the effective doping. The same trend was confirmed in our as-grown and annealed samples with 12% nominal Mn doping. In Figs. 1(d)–1(f) we highlight the observed correlation between the peak position and its height, as well as the expected correlation from the valence band theories between the amplitude of the peak and the dc conductivity. We also point out the close correspondence shown in Fig. 1(f) between the dc conductivities obtained from extrapolated THz data and from dc longitudinal and Hall transport measurements, which confirms the consistency of our optical data.

Unlike the unpolarized optical spectroscopy, the magneto-optical effects are very sensitive to the magnetic state of the system, their interpretation is more microscopically constrained, and they yield sharper spectral features. This is particularly valid for the infrared magneto-optical spectroscopy for which previous study [16] has shown that the disordered valence band theory with kinetic-exchange-split bands of ferromagnetic (Ga,Mn)As accounts semiquantitatively for the overall characteristics of the measured data. We now extend the analysis to higher energies including transitions across the semiconductor band gap.

The magnetic circular dichroism in the reflection geometry is given by $\mathrm{MCD(deg)} = 90/\pi(R^+ - R^-)/(R^+ + R^-)$, where $R^{+(-)}$ is the reflected intensity of the light with the angular momentum $+1$ (-1). The main result of MCD measurements in our (Ga,Mn)As materials, shown in Figs. 2(a) and 2(b), is the observed large blueshift of the MCD peak (the peak is negative in the above sign convention). Our data contradict the conclusion based on experiments in Ref. [9] which stated that the position of the MCD peak was independent of doping and that this was a signature of the pinning of the Fermi level in a rigid narrow impurity band [9,10]. We have also performed additional MCD experiments in pairs of as-grown and annealed (Ga,Mn)As materials. Upon annealing, we again observe a blueshift of the MCD peak, as illustrated in Fig. 2(c).

Theoretical modeling of the MCD spectra within the valence band theory, described in detail in Ref. [11], is shown in Fig. 2(d). The magnitude of the peak and its absolute position depend on the detailed implementation of the model, e.g., on the way disorder or band-gap renormalization effects are treated [11]. On a qualitative level and independent of these specific implementations of the model, the valence band theory with the antiferromagnetic

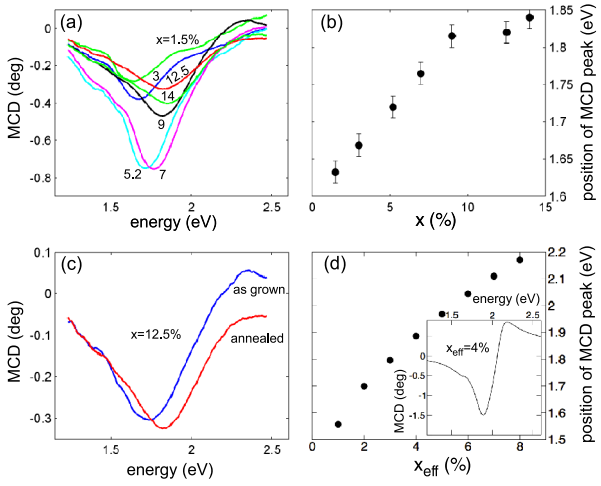

FIG. 2 (color online). (a) Reflection MCD measurements in samples from the optimized series of 20 nm thick epilayers spanning the whole studied range of Mn dopings of ferromagnetic (Ga,Mn)As. (b) Experimental position of the MCD peak (negative in the considered sign convention) as a function of nominal doping. (c) Comparison of the MCD measurements in the 12.5% doped as-grown and annealed epilayer. (d) Theoretical position of the MCD peak as a function of effective doping of uncompensated Mn_{Ga} impurities (see Ref. [11]); inset shows theoretical MCD spectrum for 4% effective doping.

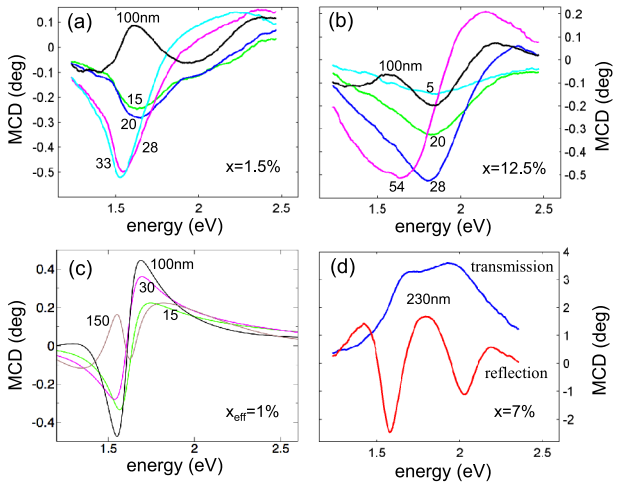

FIG. 3 (color online). Measured reflection MCD data in samples with different (Ga,Mn)As epilayer thickness and nominal Mn doping 1.5% (a), 12.5% (b). (c) Theoretical thickness dependence of the MCD spectra at 1% effective doping. (d) Transmission and reflection MCD measurements in a 7% nominally doped 230 nm thick freestanding (Ga,Mn)As epilayer.

p-d kinetic exchange [3] reproduces the overall experimental shape of the MCD spectrum, the sign of the MCD peak, and the blueshift of the peak with increasing doping.

Because our experiments were performed in the reflection geometry we have prepared several control samples to assess the role of multiple reflections. In Figs. 3(a) and 3(b) we show a comparison of MCD spectra in (Ga,Mn)As epilayers of different thicknesses controlled during growth or postgrowth by etching [11]. In the control thicker (Ga,Mn)As samples, the MCD peak is superimposed on oscillations caused by the multiple reflections. The oscillations are completely suppressed in the 20 nm thick films, and the reflection MCD peak position is therefore not affected by the film thickness in our series of optimized 20 nm thick (Ga,Mn)As epilayers. The transition from a thin film to a film where multiple reflections are important is captured qualitatively by the valence band theory calculations, as shown in Fig. 3(c).

As an additional consistency check of the sign of our MCD signals with respect to previous MCD experiments in (Ga,Mn)As we have also measured the freestanding 230 nm thick 7% Mn-doped (Ga,Mn)As epilayer in both reflection and transmission MCD geometry. In the latter case the dichroism is given by $\mathrm{MCD(deg)} = 90/\pi(T^+ - T^-)/(T^+ + T^-)$, where $T^{+(-)}$ is the transmitted intensity of the light with the angular momentum $+1$ (-1). Our transmission MCD data shown in Fig. 3(d) are very similar to measurements in samples with comparable doping and film thickness reported in Ref. [17].

To conclude, our optical spectroscopy measurements in a large set of systematically prepared (Ga,Mn)As epilayers show that doping trends reported previously in a limited number of samples and regarded as the key experimental evidence of the impurity band nature of Fermi level states are not generic and not even prevailing in ferromagnetic (Ga,Mn)As materials. The experimental foundation of the impurity band model based on these optical spectroscopies is therefore invalid, which corroborates the absence of a microscopic theory foundation of this model. In contrast, the valence band model, which is readily established from microscopic theory and from numerous previous comparisons to experiments, accounts qualitatively or semiquantitatively for the measured optical data.

We acknowledge experimental support from Duncan K. Maude and EU Grants FP7-215368 SemiSpinNet and FP7-214499 NAMASTE, Czech Republic Grants KAN400100652, LC510, MEB020928, Preamium Academiae, AV0Z10100521, MSM0021620834, MSM0021620857, GACR 202/09/H041, SVV-2010-261306 of the Charles University, and U.S. Grants NSF-MRSEC DMR-0820414, ONR-N000140610122, DMR-0547875, and SWAN-NRI. J. S. acknowledges financial support through a Cottrell Scholar Award from the Research Corporation.

[1] H. Ohno, Science **281**, 951 (1998).
[2] F. Matsukura, H. Ohno, and T. Dietl, in *Handbook of Magnetic Materials*, edited by K. H. J. Buschow (Elsevier, Amsterdam, 2002), Vol. 14, p. 1.
[3] T. Jungwirth, J. Sinova, J. Mašek, J. Kučera, and A. H. MacDonald, Rev. Mod. Phys. **78**, 809 (2006).
[4] *Spintronics*, edited by T. Dietl, D. D. Awschalom, M. Kaminska, and H. Ohmo, Semiconductors and Semimetals, Vol. 82 (Elsevier, New York, 2008).
[5] J. Mašek *et al.*, following Letter, Phys. Rev. Lett. **105**, 227202 (2010).
[6] K. S. Burch, D. D. Awschalom, and D. N. Basov, J. Magn. Magn. Mater. **320**, 3207 (2008).
[7] K. S. Burch *et al.*, Phys. Rev. Lett. **97**, 087208 (2006).
[8] P. R. Stone *et al.*, Phys. Rev. Lett. **101**, 087203 (2008).
[9] K. Ando *et al.*, Phys. Rev. Lett. **100**, 067204 (2008).
[10] J.-M. Tang and M. E. Flatté, Phys. Rev. Lett. **101**, 157203 (2008).
[11] See supplementary material at http://link.aps.org/supplemental/10.1103/PhysRevLett.105.227201 for additional information on material growth and characterization, optical experiments, and theory.
[12] W. Songprakob, R. Zallen, D. V. Tsu, and W. K. Liu, J. Appl. Phys. **91**, 171 (2002).
[13] J. Sinova *et al.*, Phys. Rev. B **66**, 041202 (2002).
[14] S. R. E. Yang *et al.*, Phys. Rev. B **67**, 045205 (2003).
[15] T. Jungwirth *et al.*, Phys. Rev. B **76**, 125206 (2007).
[16] G. Acbas *et al.*, Phys. Rev. Lett. **103**, 137201 (2009).
[17] B. Beschoten *et al.*, Phys. Rev. Lett. **83**, 3073 (1999).